Online Optimization of Zero-Sequence Voltage Injection of PWM Strategy for 3L-NPC converters

Novak, Mateja; Sangwongwanich, Ariya; Blaabjerg, Frede

Published in:
Proceedings of the 2022 International Power Electronics Conference (IPEC-Himeji 2022- ECCE Asia)

DOI (link to publication from Publisher):
10.23919/IPEC-Himeji2022-ECCE53331.2022.9807087

Publication date:
2022

Document Version
Accepted author manuscript, peer reviewed version

Online Optimization of Zero-Sequence Voltage Injection of PWM Strategy for 3L-NPC converters

Mateja Novak*, Ariya Sangwongwanich and Frede Blaabjerg
AAU Energy, Aalborg University, Aalborg, Denmark
*E-mail: nov@energy.aau.dk

***Abstract*—Various pulse-width modulation (PWM) methods have been proposed to improve the control performance of three-phase three-level neutral-point clamped (3L-NPC) converters. However, the state-of-the-art PWM methods usually have a trade-off between switching losses and neutral-point (NP) voltage balancing performance. In practical applications, different control objectives should be prioritized according to the operating conditions of the power converter. In that case, the existing PWM methods cannot ensure optimum control performance of the power converter when the operating conditions (e.g. modulation index, power factor and output frequency) vary in a wide range. In this paper, an algorithm for online optimization of the zero-sequence voltage injection (ZVI) is proposed. The proposed method can prioritize different control objectives and select the most suitable PWM method based on the operating point without any parameter adjustment. The obtained results have validated that a combination of different ZVI methods can provide an optimum trade-off between the switching losses and NP voltage fluctuations for different converter operating conditions.**

***Index Terms*—Neutral Point Clamped Converter, Voltage Balancing, PWM, Optimization, Zero Sequence Voltage Injection**

I. Introduction

Key performance metrics of 3L-NPC converters such as efficiency, reliability, voltage balancing, and power quality are strongly dependent on the applied PWM technique [1]–[3]. Therefore, several PWM methods have been proposed for the 3L-NPC topology to address certain aspects [4]. When implementing the PWM method with a carrier-based PWM (CB-PWM) approach, the main difference among the PWM methods is related to the selection of the zero-sequence voltage injection (ZVI) method [5], [6].

The PWM methods proposed for 3L-NPC topology shown in Fig. 1 can generally be classified into two groups according to their main control objective: 1) minimizing the number of switching transition and 2) minimizing the NP voltage fluctuation. In the first category, the aim of the PWM strategy is to reduce the switching loss in the power devices by reducing the number of switching transitions in a switching period [7]–[9]. By doing so, the efficiency of the power converter can be improved. This is usually achieved by utilizing the nearest-three-vectors (NTV) around the reference voltage in the space vector diagram. The NTV-PWM method can be implemented with either continuous or discontinuous modulation schemes [10]. The former one generally offers better power quality performance while the latter one ensure minimum number of switching transition. However, both NTV-PWM methods do not contribute to the NP voltage balancing and thus can result in a large NP voltage oscillation.

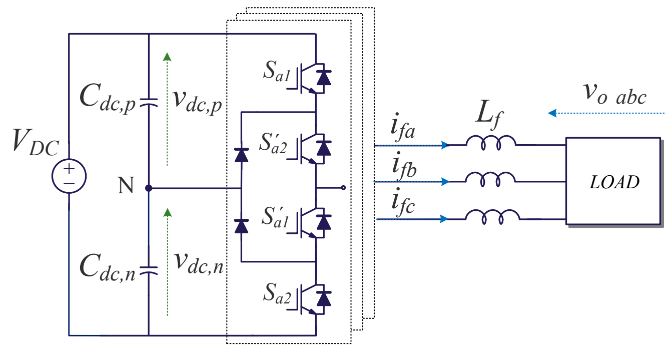

Fig. 1: Topology of the three-phase three level NPC converter.

The NP voltage fluctuation is an inherent issue of the NPC topology, which can lead to over-voltage of the components (e.g., power devices and dc-link capacitors), if not being regulated. Therefore, the second category of the developed PWM methods aims to solve this issue. One very effective PWM method to eliminate the NP voltage fluctuation is the nearest-three-virtual-vector (NTV^2) approach [11], [12]. In the NTV^2-PWM approach, three virtual vectors are created from a combination of the voltage vectors, which have complementary impact on the flow of NP current. Therefore, when applying each of the virtual voltage vectors, it can be ensured that the average NP current will be zero and thus the NP voltage fluctuation will be fully eliminated. However, the trade-off in this approach is the increased number of switching transitions, which leads to higher switching losses.

According to the above discussion, there is a trade-off when applying a certain PWM method. Ideally, the selection of the PWM strategy should be optimized considering the operating conditions [13]. For instance, reducing the switching loss is crucial when the power converter operates close to the rated power. In that case, the NTV-PWM approach is a suitable PWM method to be applied to ensure high efficiency. On the other hand, when the AC output frequency of the power converter decreases, the NP voltage fluctuation will be more severe (e.g., during low-speed operation of motors). In that case, the NTV^2-PWM method should be applied to mitigate this issue. However, there are several applications where the operating condition of the power converter (e.g., modulation index, power factor and output frequency) can vary in a

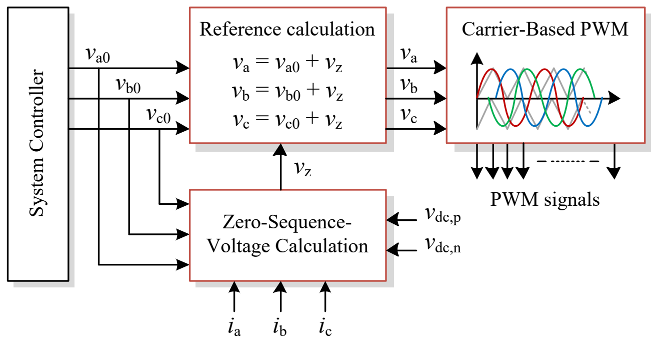

Fig. 2: Control diagram of pulse-width modulation technique with zero-sequence voltage injection for 3L-NPC converters.

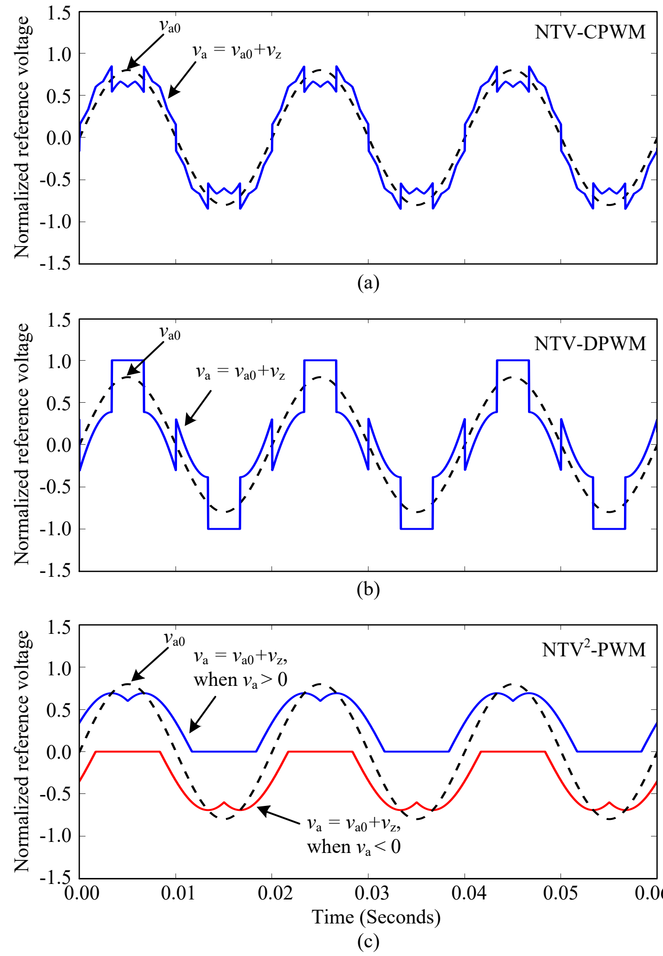

Fig. 3: Implementation of CB-PWM technique based on: a) NTV-CPWM, b) NTV-DPWM, and c) NTV^2-PWM methods, where v_{a0} and v_a are the reference voltage before and after adding the zero-sequence voltage v_z.

wide range during the operation such as variable-speed drive application. In those cases, it is challenging to adaptively apply the most suitable PWM method and optimize the power converter performance during the entire operation.

In this paper, a method to provide online optimization of zero-sequence voltage selection is proposed. The proposed method evaluates the impact of the switching loss and NP voltage balancing of different ZVI methods online and then selects the most suitable ZVI method based on defined cost function. By doing so, the optimal ZVI method can be adaptively selected according to the current operating conditions. The structure of the paper is as follows. In Section II three different ZVI methods are introduced. The working principle of the proposed optimized zero-sequence voltage injection (OP-ZVI) is explained in Section III. The analysis of effects of the ZVI methods on the switching losses and NP voltage fluctuation and experimental validation are provided in Section IV. Section V concludes the article.

II. Zero-Sequence Voltage Injection Methods

The zero-sequence voltage v_z, which is added to all the three-phase reference voltage, provides a degree of freedom to effectively utilize different vector combinations in CB-PWM methods. Various PWM methods can be created by using different methods for calculating the zero-sequence voltage v_z, as it is illustrated in Fig. 2.

A. Nearest-Three-Vector Continuous PWM (NTV-CPWM)

The NTV PWM approach can be implemented with continuous modulation schemes, as it was proposed in [7]–[9]. In this method, two redundant voltage vectors are employed in each area of the sector. This method corresponds to the space vector modulation (SVM) when using four vectors with six switching transitions within one switching cycle.

An example waveform of reference voltage for NTV-CPWM method with CB-PWM implementation is shown in Fig. 3(a), where it can be seen that there is no clamping period in any of the phases during operation. In comparison with the other PWM strategies, NTV-CPWM method provides a better power quality performance with lower THD in the output voltage under the same power loss conditions [4]. However, since the method does not contribute to the NP balancing, low-frequency oscillation are visible in NP voltage.

B. Nearest-Three-Vector Discontinuous PWM (NTV-DPWM)

The NTV PWM method can also be implemented with a discontinuous PWM scheme [10]. Compared to NTV-CPWM, the number of voltage vectors used within one switching cycle is reduced to three. Moreover, as it is shown in Fig. 3(b), one of the phase voltages is clamped at either positive or negative dc-bus. Consequently, the switching loss can be reduced compared to the NTV-CPWM method.

However, while clamping the phase voltage has a positive effect on reduction of the switching loss, it has a negative effect on the power quality of the output waveform (e.g., resulting in higher THD). Furthermore, a relatively high amplitude of the low-frequency oscillation in the NP voltage can be observed, which is a trade-off using this PWM method.

C. Nearest-Three-Virtual-Vector PWM (NTV^2-PWM)

The nearest-three-virtual-vector PWM method which can fully eliminate the NP voltage variation over the wide range of operating conditions (e.g., modulation index and power factor) was proposed in [11], [12]. The concept of virtual vectors is achieved by using a combination of redundant vectors, which have complementary effects on the NP current. In this way, the average NP current, when virtual vectors from the NTV^2-PWM method are used, is essentially equal to zero.

The NTV^2-PWM method can be implemented by decomposing the phase reference voltage v_{x} into the reference for the upper v_{xp} and low v_{xn} carrier as shown in Fig. 3(c). Since the average NP current is forced to be zero in every switching cycle, no low-frequency variations in the NP voltage exist. However, this method increases the number of switching transition and thus the switching losses are higher than for the other CB-PWM methods.

III. Proposed Optimized Zero-Sequence Voltage Injection (OP-ZVI) PWM Method

The aim of the proposed optimized zero-sequence voltage injection (OP-ZVI) method is to determine the optimum ZVI technique based on the required performance metrics, which can be defined as a cost function. For instance, a cost function, which ensures a good trade-off between the low switching losses and low NP voltage fluctuation can be formulated as:

$$cost = \lambda \cdot \Delta N_{sw}(k+1) \cdot f_n + (1-\lambda) \cdot \Delta v_{NP}(k+1) \cdot I_n \quad (1)$$

where $\lambda \in [0,1]$ is the weighting factor, Δv_{NP} is the amplitude of the NP voltage variation, I_n is the amplitude of the output current, ΔN_{sw} is the number of switching transitions, and f_n is the frequency of the output current (all parameters are normalized). The cost function parameters include both the converter operating conditions (i.e., I_n and f_n) and the consequence of the ZVI technique (i.e., Δv_{NP} and ΔN_{sw}). This implies that:

- The cost function is self-adjusting according to the current operating condition of the power converter.
- The impact of different ZVI techniques can be evaluated with the cost function.

The proposed OP-ZVI employs similar idea as a finite-set model predictive algorithm, where the parameters in the cost function (i.e., Δv_{NP} and ΔN_{sw}) are first predicted for each ZVI technique. Then, the cost function is evaluated to find the optimum ZVI technique, which offers the minimum value following the work-flow in Fig. 4.

A. Parameters Estimation

It is crucial to determine the impact of different ZVI methods on the NP voltage variation Δv_{NP} and number of switching transition ΔN_{sw} in the cost function. The prediction of NP voltage variation Δv_{NP} can be obtained by first estimating the average NP current following [14]:

$$\begin{aligned} i_{\mathrm{NP}}(k+1) \;=\; & -(\mathrm{s}(v_{\mathrm{a}}) \cdot v_{\mathrm{a0}} i_{\mathrm{a}} + \mathrm{s}(v_{\mathrm{b}}) \cdot v_{\mathrm{b0}} i_{\mathrm{b}} + \mathrm{s}(v_{\mathrm{c}}) \cdot v_{\mathrm{c0}} i_{\mathrm{c}}) \\ & - v_{\mathrm{z}}(\mathrm{s}(v_{\mathrm{a}}) \cdot i_{\mathrm{a}} + \mathrm{s}(v_{\mathrm{b}}) \cdot i_{\mathrm{b}} + \mathrm{s}(v_{\mathrm{c}}) \cdot i_{\mathrm{c}}) \end{aligned} \quad (2)$$

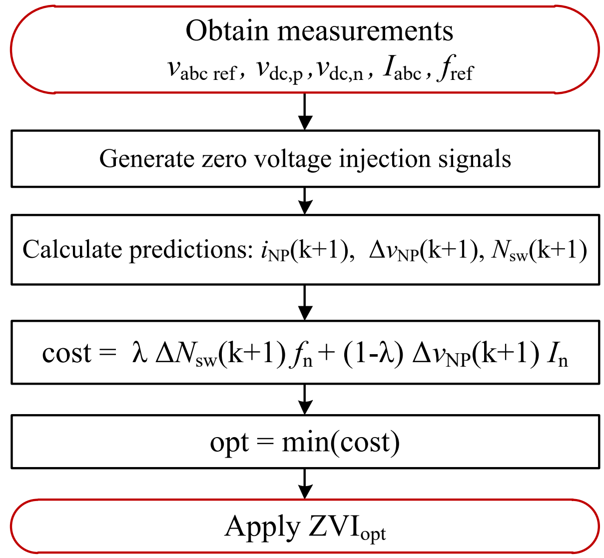

Fig. 4: Workflow of the proposed OP-ZVI method.

where $\mathrm{s}(v_{\mathrm{x}})$ indicates the sign function, which has a value of either 1 or -1 for positive and negative value of v_{x}, respectively. The obtained NP current prediction is afterwards used to calculate the NP voltage fluctuation as:

$$\Delta v_{NP}(k+1) \;=\; (i_{NP}(k+1) \cdot T_s)/C_{dc} \quad (3)$$

where T_s is the switching period and C_{dc} is the capacitance of the DC-link capacitors.

Thus, when applying different zero-sequence voltage v_{z} in (2), the prediction of the NP voltage fluctuation (in the next sampling) $\Delta v_{NP}(k+1)$ in (3) of each ZVI method can be determined. The same approach can also be applied to estimate ΔN_{sw} for each ZVI method by considering the sign changing of the references in the upper and lower carriers.

B. Weighting Factor

The use of weighing factor λ in the cost function (1) offers another degree of freedom to prioritize the NP voltage balancing performance and switching loss. From the cost function, it can be observed that for $\lambda < 0.5$ the main objective of optimization will be minimization of the NP voltage fluctuation, while for $\lambda > 0.5$ the algorithm will prioritize the minimization of the switching losses. Values of I_n and f_n also provide the feedback to the algorithm about the converter operating point and are used to adapt the ZVI signal to the operating point of the converter. The logic is the following: for high converter currents, the optimization will prioritize the minimization of switching losses, while for low frequencies it will prioritize the minimization of NP voltage fluctuation.

IV. Results

The proposed methods will be evaluated on 3L-NPC converter system with an output filter and a resistive load as shown in Fig. 1. The system parameters are given in Table

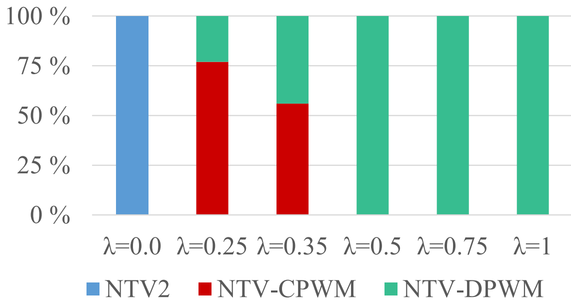

(a) For f_{ref} = 50 Hz.

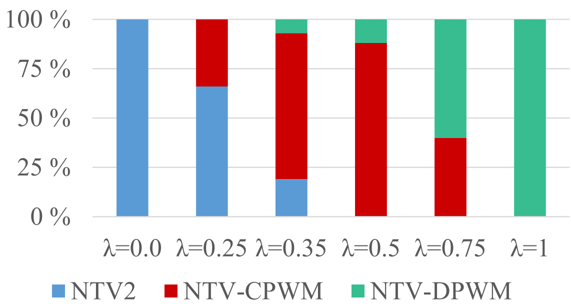

(b) For f_{ref} = 10 Hz.

Fig. 5: Utilization of ZVI techniques during one switching perido (%) in the proposed OP-ZVI method depending on the selected weighting factor value λ for m_a = 0.9 .

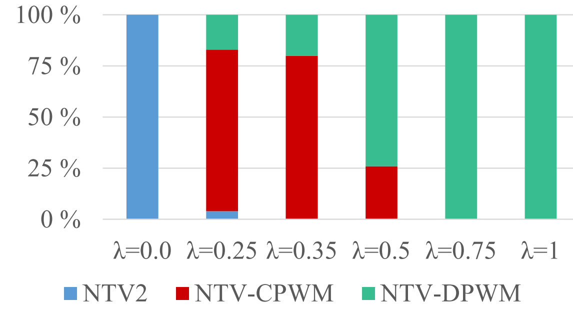

(a) For f_{ref} = 50 Hz.

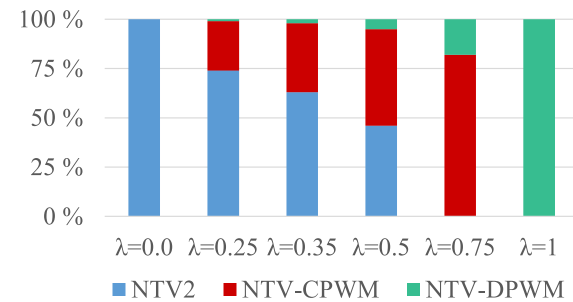

(b) For f_{ref} = 10 Hz.

Fig. 6: Utilization of ZVI techniques during one switching perido (%) in the proposed OP-ZVI method depending on the selected weighting factor value λ for m_a = 0.5.

TABLE I: Parameters of the 3L-NPC converter system.

Description	Parameter	Value
DC-link voltage	V_{DC}	700 V
DC-link capacitors	$C_{dc,p}$, $C_{dc,n}$	4.1 mF
Output filter	L_f	1.2 mH
Switching frequency	f_{sw}	5 kHz
Load	R_{load}	5 Ω
Nominal current	I_{nom}	100 A

I and the devices were modelled in PLECS using the data sheet values provided by the manufacturer [15]. Four converter operating points with different combination of modulation index (m_a) and AC output frequency (f_{ref}) will be included in the analysis:

1) m_a = 0.9 and f_{ref} = 50 Hz
2) m_a = 0.9 and f_{ref} = 10 Hz
3) m_a = 0.5 and f_{ref} = 50 Hz
4) m_a = 0.5 and f_{ref} = 10 Hz

A. Effects on the switching losses and NP voltage fluctuation

The simulation results of the 3L-NPC converter operated with the NTV-CPWM, the NTV-DPWM, the NTV^2, and the proposed methods for different weighting factor values are carried out. A comparison of the utilization of the ZVI methods is shown in Fig. 5 and Fig. 6. It can be observed that for $\lambda > 0.5$, m_a = 0.9 and f_{ref} = 50 Hz, the proposed OP-ZVI method mostly employs the NTV-DPWM method. This can ensure that the switching losses are minimized, which is preferable when operating at high loading condition (e.g., high modulation index). It is also interesting to observe that using $\lambda = 0.35$ in that operating point results in an equal utilization of NTV-DPWM and NTV-CPWM methods and it leads to a good trade-off of performance with 64 W of switching losses and 5.4 V amplitude of NP ripple as shown in Fig. 7.

On the other hand, for the operating point m_a = 0.9 and f_{ref} = 10 Hz, NTV-DPWM is no longer an optimum choice since it will cause a very high NP voltage fluctuations as shown in Fig. 8. In this case, a combination of NTV-CPWM and NTV-DPWM is used to ensure a good trade-off between the two objectives. It can also be observed that the operating points m_a = 0.9 and f_{ref} = 10 Hz and m_a = 0.5 and f_{ref} = 50 Hz for $\lambda = 0.5$ are complementary in terms of utilization of NTV-DPWM and NTV-CPWM methods. Moreover, in Fig. 5b and Fig. 6a it can be observed that the switching losses are two times higher for m_a = 0.9 and f_{ref} = 10 Hz if NTV^2-PWM is used in both cases or if NTV-DPWM is used for both operating points, then the NP ripple is seven times higher. Finally, the last operating point m_a = 0.5 and f_{ref} = 10 Hz shows that a combination of all three methods is used in Fig. 6b. Although the selected cases are border operating points examples, they show a clear indication that for the m_a and f_{ref} values that fit between these border cases, OP-ZVI method will combine all three ZVI methods.

A simulation was also conducted for AC output frequency change during high current operation as shown in Fig. 11. It

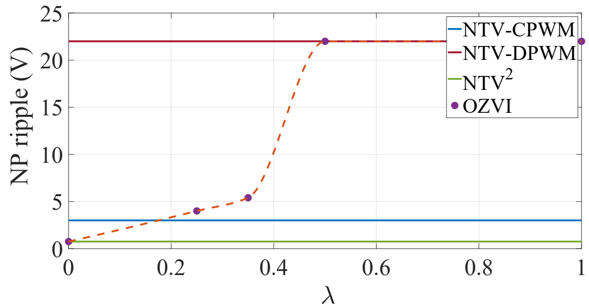

(a) NP voltage fluctuation.

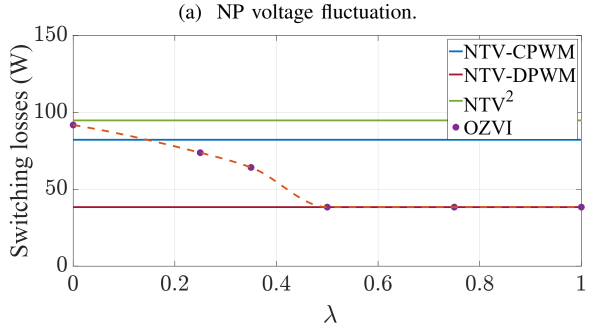

(b) Converter switching losses.

Fig. 7: Comparison of the conventional control methods and proposed OP-ZVI method for high modulation index (I = 100 A, m_a = 0.9) and high frequency (50 Hz).

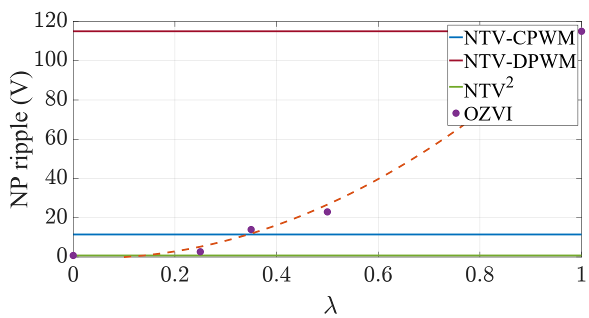

(a) NP voltage fluctuation.

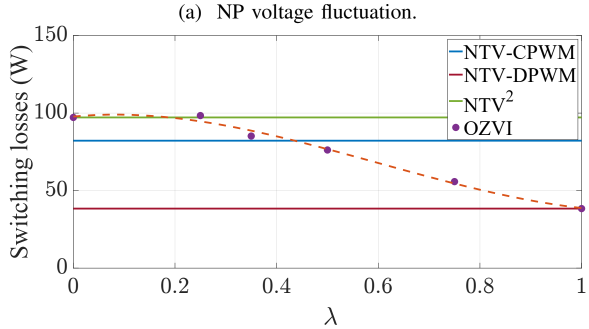

(b) Converter switching losses.

Fig. 8: Comparison of the conventional control methods and proposed OP-ZVI method for high modulation index (I = 100 A, m_a = 0.9) and low frequency (10 Hz).

can also be observed how during the transient operation the OP-ZVI method maintained the NP voltage fluctuation below 10% of the DC-link voltage. The switching loss comparison of the 3L-NPC converter for the same operating conditions is provided in Table II. The comparison shows that the OP-ZVI

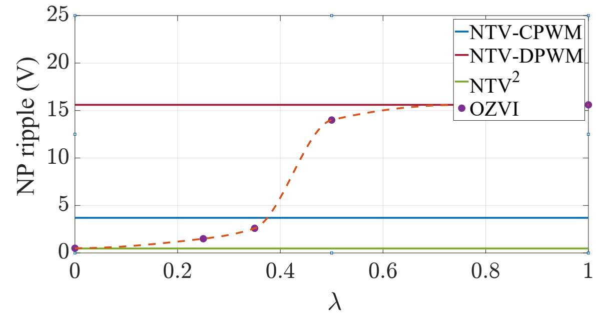

(a) NP voltage fluctuation.

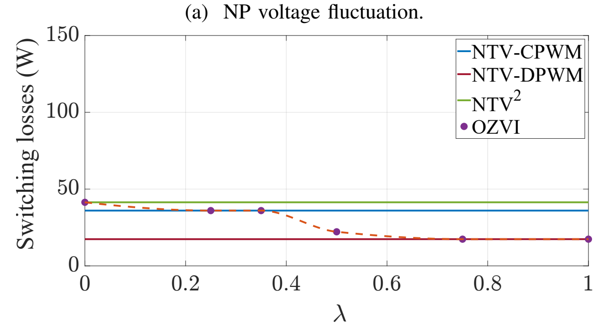

(b) Converter switching losses.

Fig. 9: Comparison of the conventional control methods and proposed OP-ZVI method for high modulation index (I = 55 A, m_a = 0.5) and high frequency (50 Hz).

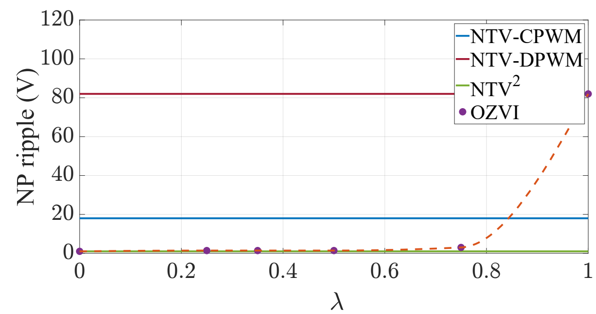

(a) NP voltage fluctuation.

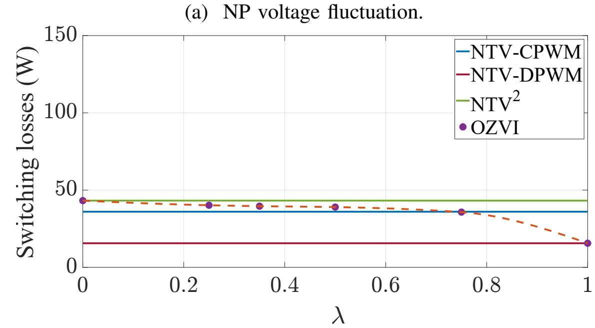

(b) Converter switching losses.

Fig. 10: Comparison of the conventional control methods and proposed OP-ZVI method for low modulation index (I = 55 A, m_a = 0.5) and low frequency (10 Hz).

method will provide lower switching losses than the NTV-CPWM and NTV^2 methods for both AC output frequencies.

B. Experimental results

Experimental tests have been carried out with the 3L-NPC converter prototype and the NP voltage fluctuation was

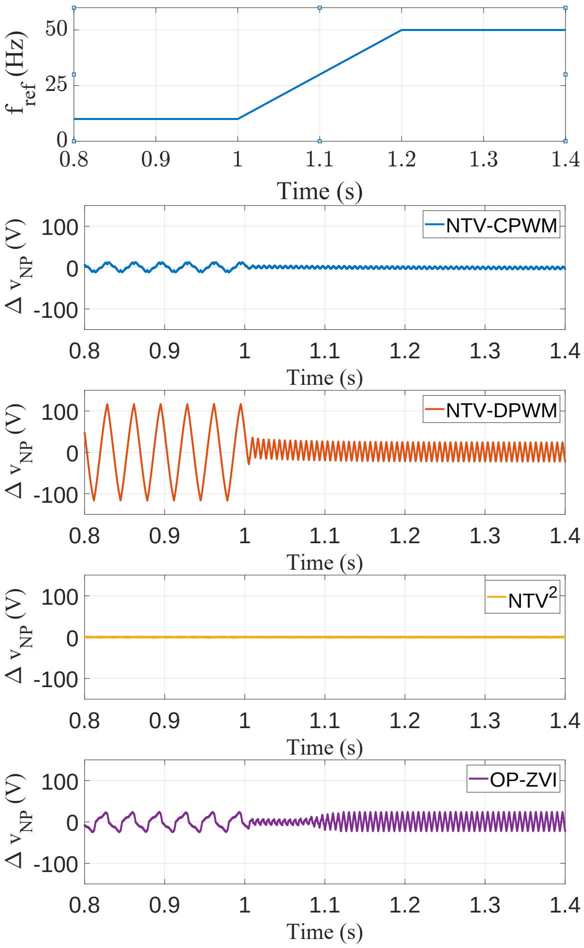

Fig. 11: Comparison of the NP voltage fluctuation for ZVI methods during f_{ref} change from 10 → 50 Hz (m_a = 0.9). Load is constant.

evaluated for different ZVI methods. The test were performed for low modulation index ($m_a = 0.6$) and low reference frequency (f_{ref} = 10 Hz). The waveform in Fig. 12 shows the case when λ in OP-ZVI method is set to 1 and 0, which means the OP-ZVI is applying the DPWM and NTV^2, respectively. It is observed that NTV^2 can provide the lowest NP voltage fluctuation, while for NTV-DPWM the fluctuation is much larger and the load current shows distortion. Afterwards, λ was set to 0.5 and the experiments were repeated for the same operating point. The analysis in the previous section showed that for this operating point the OP-ZVI will combine the ZVI signals of DPWM and NTV-CPWM to obtain a good trade off between low NP voltage fluctuation and low switching losses. Obtained waveforms show a much lower NP voltage fluctuation than NTV-DPWM and less distorted current waveforms.

V. Conclusion

An algorithm to optimally select the zero-sequence voltage of a 3L-NPC converter according to its operating conditions is proposed. For high modulation index, the proposed method will prioritize the minimization of switching losses, where the NTV-DPWM method is mostly utilized while the NTV^2-PWM method will be employed under low AC output frequency condition to minimize the NP voltage fluctuation. Therefore, it can be used to ensure an optimum trade-off between the switching losses and NP voltage fluctuation.

TABLE II: Switching losses of the 3L-NPC converter for different f_{ref} and m_a = 0.9.

PWM method	$P_{sw,\ 50Hz}$	$P_{sw,\ 10Hz}$
NTV-CPWM	82 W	82 W
NTV-DPWM	40 W	40 W
NTV^2	100 W	100 W
OP-ZVI	40 W	76 W

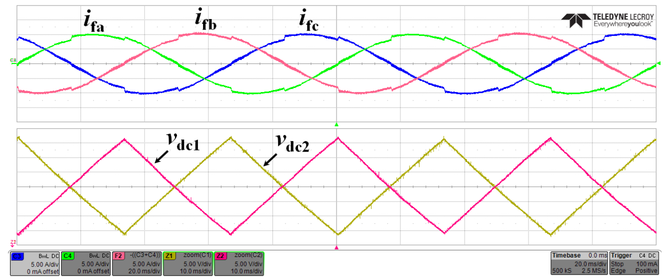

(a) For λ = 1 (NTV-DPWM).

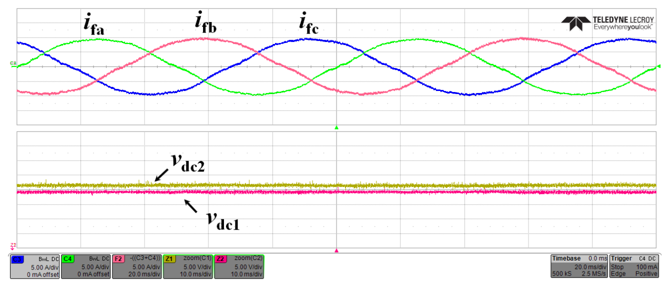

(b) For λ = 0 (NTV^2).

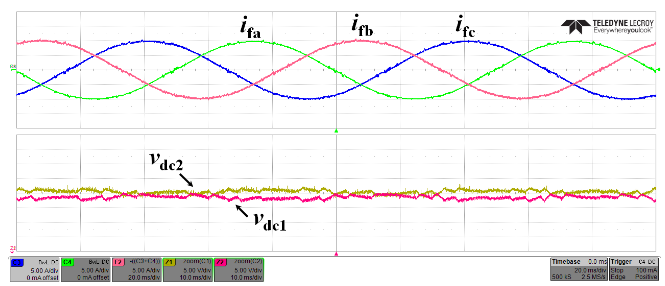

(c) For λ = 0.5 (OP-ZVI).

Fig. 12: Measured output currents and DC-link voltages of the 3L-NPC converter operating with different ZVI methods for V_{DC} = 550 V, f_{ref} = 10 Hz, m_a = 0.6.

Acknowledgments

The work is supported by the Reliable Power Electronic-Based Power System (REPEPS) project at the AAU Energy, Aalborg University as a part of the Villum Investigator Program funded by the Villum Foundation.

REFERENCES

[1] J. Rodriguez, S. Bernet, P. K. Steimer, and I. E. Lizama, "A survey on neutral-point-clamped inverters," *IEEE Trans. Ind. Electron.*, vol. 57, no. 7, pp. 2219–2230, 2010.

[2] A. Nabae, I. Takahashi, and H. Akagi, "A new neutral-point-clamped PWM inverter," *IEEE Trans. on Ind. App.*, vol. IA-17, no. 5, pp. 518–523, 1981.

[3] N. Celanovic and D. Boroyevich, "A comprehensive study of neutral-point voltage balancing problem in three-level neutral-point-clamped voltage source PWM inverters," *IEEE Tran. Power Electron.*, vol. 15, no. 2, pp. 242–249, 2000.

[4] T. Bruckner and D. Holmes, "Optimal pulse-width modulation for three-level inverters," *IEEE Trans. Power Electron.*, vol. 20, no. 1, pp. 82–89, 2005.

[5] W. Yao, H. Hu, and Z. Lu, "Comparisons of space-vector modulation and carrier-based modulation of multilevel inverter," *IEEE Trans. Power Electron.*, vol. 23, no. 1, pp. 45–51, 2008.

[6] S. Sangwongwanich and S. Paiboon, "Carrier-based realization of arbitrary space-vector PWM methods for three-level inverters," in *Proc. IPEC-ECCE Asia*, pp. 1642–1648, 2018.

[7] Y.-H. Lee, D.-H. Kim, and D.-S. Hyun, "Carrier based SVPWM method for multi-level system with reduced HDF," in *Proc. IEEE Industrial Applications Soc. Annu. Meeting*, vol. 3, pp. 1996–2003, 2000.

[8] J. Pou, R. Pindado, D. Boroyevich, and P. Rodriguez, "Evaluation of the low-frequency neutral-point voltage oscillations in the three-level inverter," *IEEE Trans. Ind. Electron.*, vol. 52, no. 6, pp. 1582–1588, 2005.

[9] D.-P. Cao, W.-X. Song, H. Xi, G.-c. Chen, and C. Chen, "Research on zero-sequence signal of space vector modulation for three-level neutral-point-clamped inverter based on vector diagram partition," in *IEEE 6th Int. Power Electron. Motion Control Conf.*, pp. 1435–1439, 2009.

[10] L. Helle, S. Munk-Nielsen, and P. Enjeti, "Generalized discontinuous dc-link balancing modulation strategy for three-level inverters," in *Proc. Power Conversion Conf.*, vol. 2, pp. 359–366, 2002.

[11] S. Busquets-Monge, J. Bordonau, D. Boroyevich, and S. Somavilla, "The nearest three virtual space vector PWM - a modulation for the comprehensive neutral-point balancing in the three-level NPC inverter," *IEEE Power Electronics Letters*, vol. 2, no. 1, pp. 11–15, 2004.

[12] J. Pou, J. Zaragoza, P. Rodriguez, S. Ceballos, V. M. Sala, R. P. Burgos, and D. Boroyevich, "Fast-processing modulation strategy for the neutral-point-clamped converter with total elimination of low-frequency voltage oscillations in the neutral point," *IEEE Trans. Ind. Electron.*, vol. 54, no. 4, pp. 2288–2294, 2007.

[13] S. Calligaro, F. Pasut, R. Petrella, and A. Pevere, "Modulation techniques for three-phase three-level npc inverters: A review and a novel solution for switching losses reduction and optimal neutral-point balancing in photovoltaic applications," in *Proc. IEEE Applied Power Electronics Conf.*, pp. 2997–3004, 2013.

[14] Q. Song, W. Liu, Q. Yu, X. Xie, and Z. Wang, "A neutral-point potential balancing algorithm for three-level npc inverters using analytically injected zero-sequence voltage," in *Proc. IEEE Applied Power Electronics Conf.*, vol. 1, pp. 228–233, 2003.

[15] *3-Level NPC IGBT-Module: SKiiP 28MLI07E3V1 datasheet*, Semikron, 6 2016, rev. 1.0.